

Supplementary Materials for

ATP Inhibits the Generation and Function of Regulatory T Cells Through the Activation of Purinergic P2X Receptors

Ursula Schenk, Michela Frascoli, Michele Proietti, Robert Geffers, Elisabetta Traggiai, Jan Buer, Camillo Ricordi, Astrid M. Westendorf, Fabio Grassi*

*To whom correspondence should be addressed. E-mail: fabio.grassi@irb.unisi.ch

Published 1 March 2011, *Sci. Signal.* **4**, ra12 (2011)

DOI: 10.1126/scisignal.2001270

The PDF file includes:

- Fig. S1. Increased suppressive function of $p2rx7^{-/-}$ T_{regs}.
- Fig. S2. Correlation between extent of ERK phosphorylation and variations in intracellular ATP concentration.
- Fig. S3. Impaired phosphorylation of ERK in $p2rx7^{-/-}$ T_{regs}.
- Fig. S4. Increases in intracellular ATP concentration and *Rorc* mRNA abundance in T_{regs} correlate with TCR signal strength.
- Fig. S5. P2X7-mediated expression of *Il17a* in T_{regs}.
- Fig. S6. Conversion of T_{conv} cells to T_{regs} by P2X antagonism.
- Fig. S7. Generation of T_{regs} by oATP and the additive effect of TGF- β .
- Fig. S8. Effects of TGF- β and oATP on the expression of genes whose products interact within the TGF- β pathway.

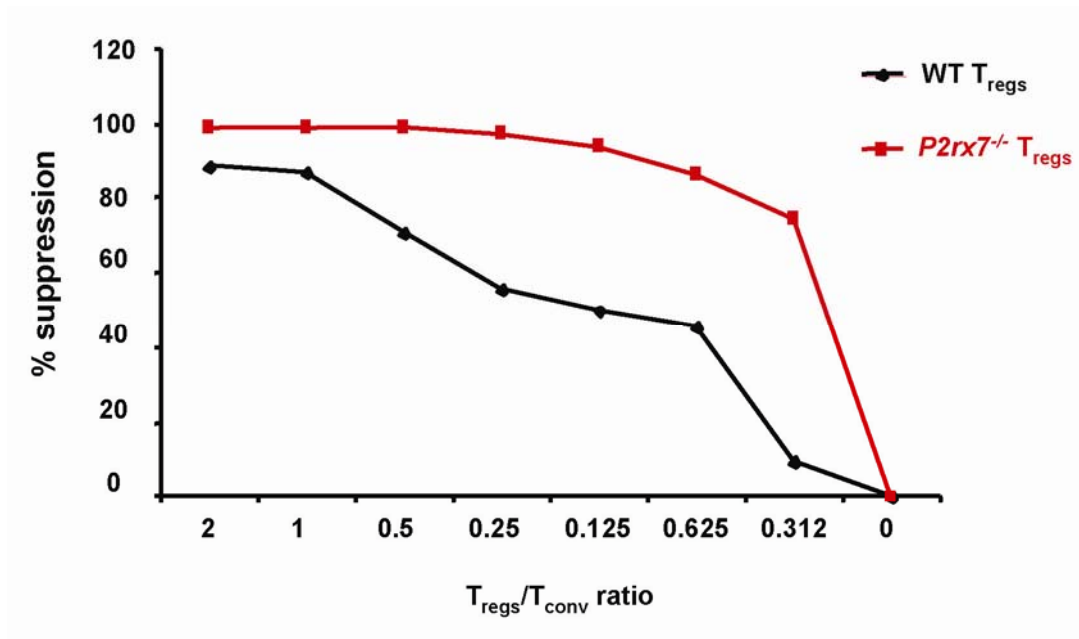


Fig. S1. Increased suppressive function of *p2rx7*^{-/-} T_{regs}. Suppression assays were performed with wild-type (WT, black line) or *p2rx7*^{-/-} (red line) T_{regs} and WT responder T_{conv} cells. Cell proliferation was determined by measurement of ³H-thymidine incorporation. Data are representative of five experiments.

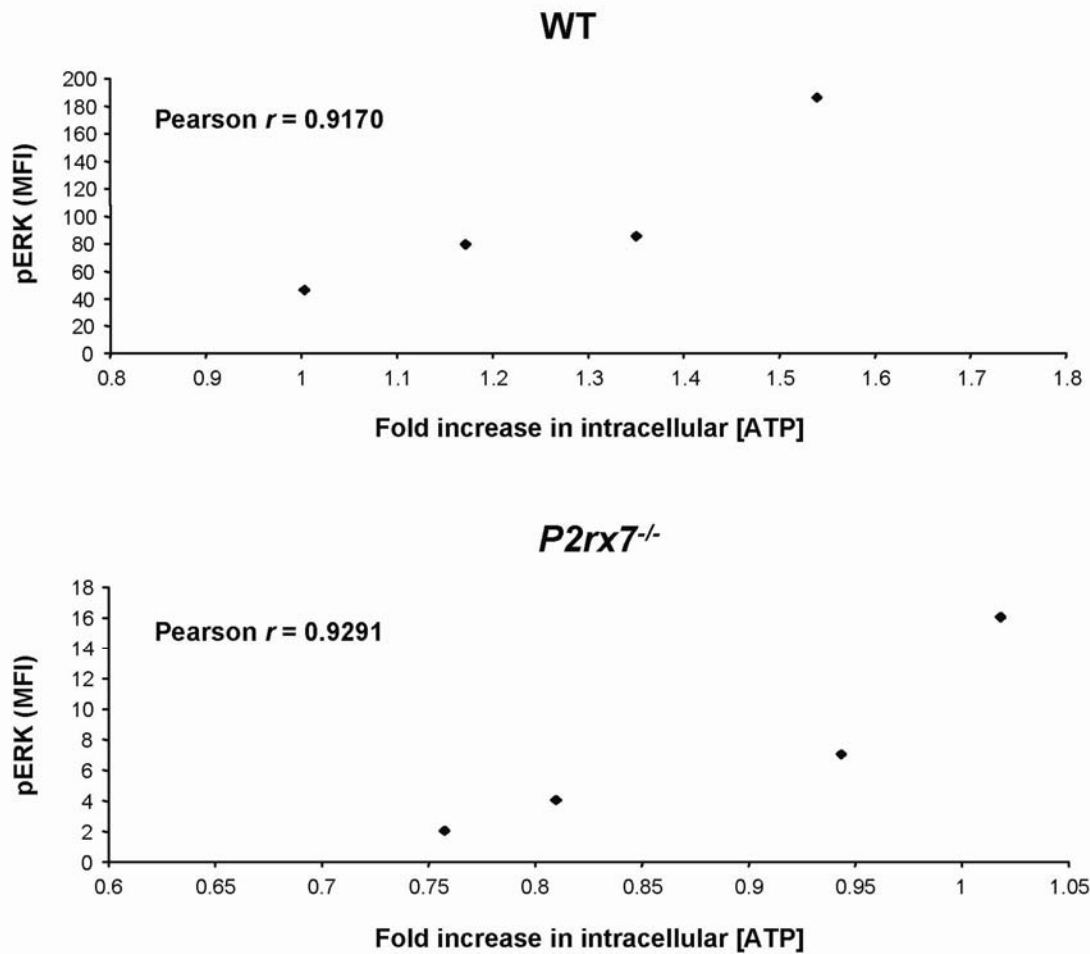


Fig. S2. Correlation between extent of ERK phosphorylation and variations in intracellular ATP concentration. WT and $p2rx7^{-/-}$ T_{regs} were stimulated for 90 min with monoclonal antibody against CD3 alone or in the presence of IL-6. ERK phosphorylation was determined by flow cytometry and expressed as the mean fluorescence intensity (MFI). The extent of phosphorylation of ERK correlated with the concentration of intracellular ATP, which was expressed as the fold-increase with respect to baseline amounts. The degree of correlation was measured by the Pearson coefficient.

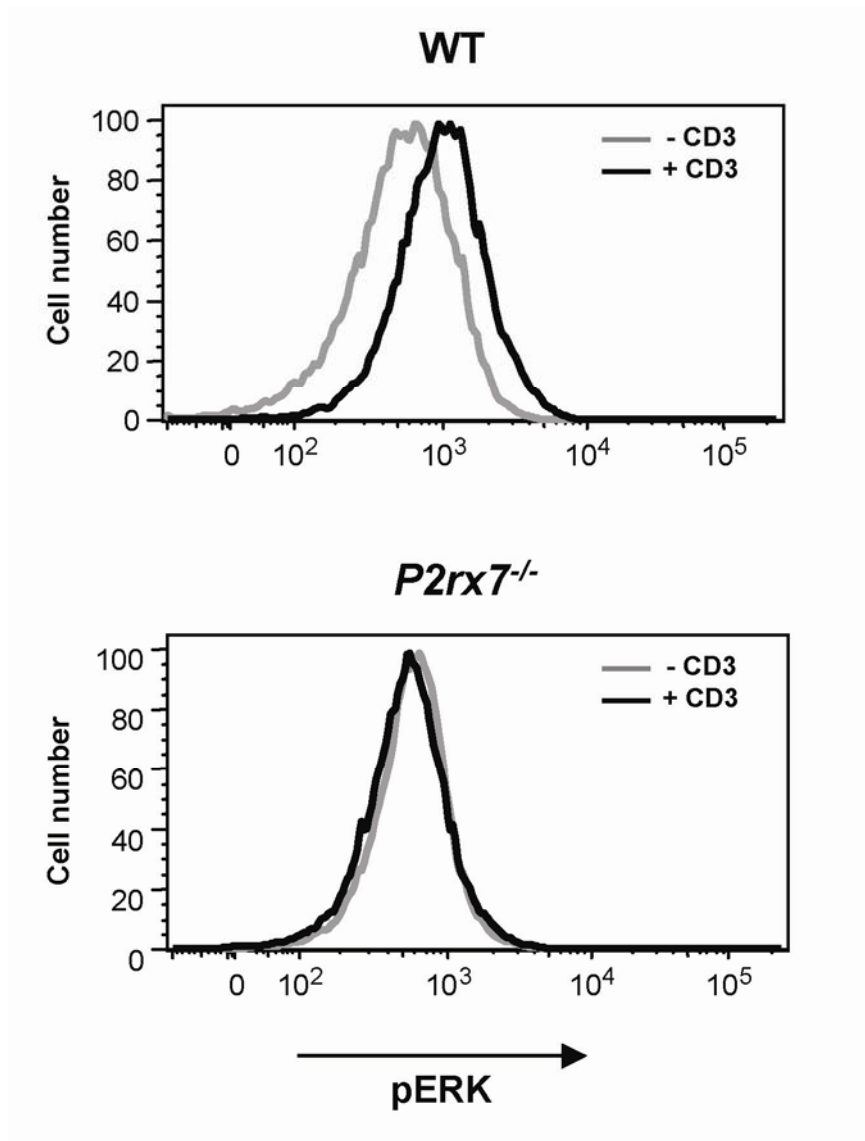


Fig. S3. Impaired phosphorylation of ERK in *p2rx7*^{-/-} T_{regs}. Flow cytometric analysis with a monoclonal antibody against pERK of sorted T_{regs} from C57BL/6 and *p2rx7*^{-/-} mice that were either unstimulated or stimulated with monoclonal antibody against CD3 for 90 min in the presence of irradiated splenocytes from *cd3ε*^{-/-} mice. Data are representative of three experiments.

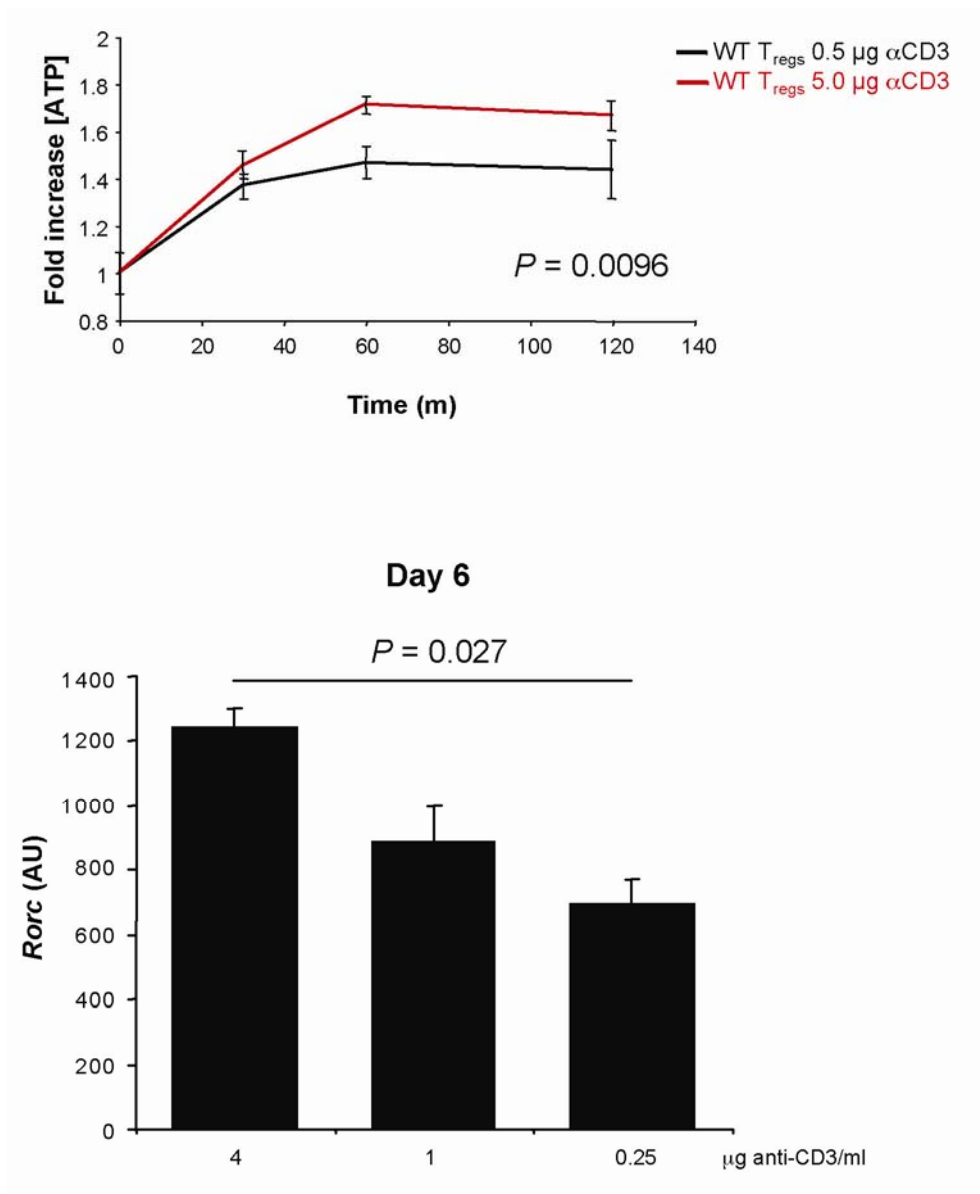


Fig. S4. Increases in intracellular ATP concentration and *Rorc* mRNA abundance in T_{regs} correlate with TCR signal strength. (Top) Variations in intracellular ATP concentration by stimulation of sorted WT T_{regs} with 0.5 μg/ml (black lines) or 5 μg/ml (red lines) of monoclonal antibody against CD3. *P* values were determined by ANOVA. (Bottom) RT-PCR analysis of the abundance of *Rorc* mRNA from WT T_{regs} stimulated for 6 days in the presence of the indicated concentrations of monoclonal antibody against CD3. Mean values ± SE are displayed (n = 3 experiments).

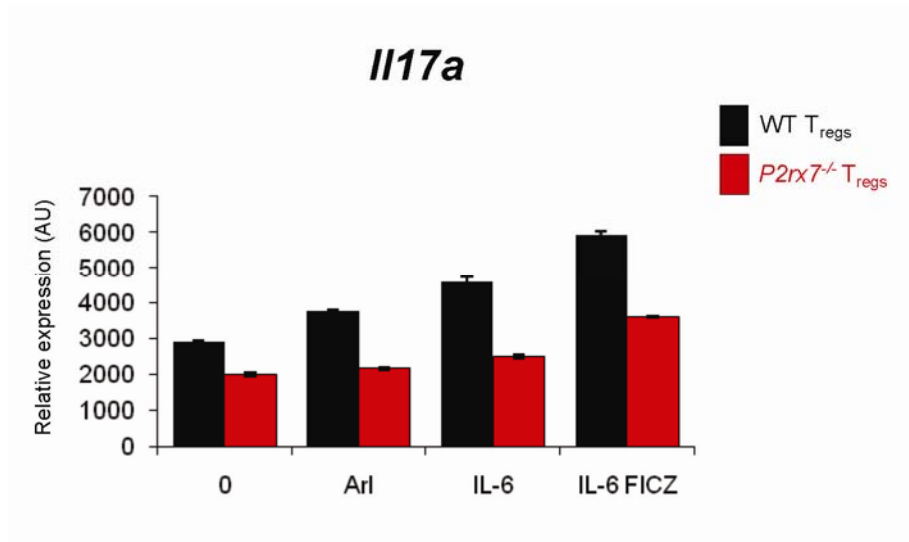


Fig. S5. P2X7-mediated expression of *Il17a* in T_{regs}. RT-PCR analysis of the abundance of *Il17a* mRNA from WT (black bars) and *p2rx7*^{-/-} (red bars) T_{regs} that were stimulated for 96 hours in the presence of ARL, IL-6, or IL-6 and FICZ. One representative experiment of two experiments is shown. AU, arbitrary units.

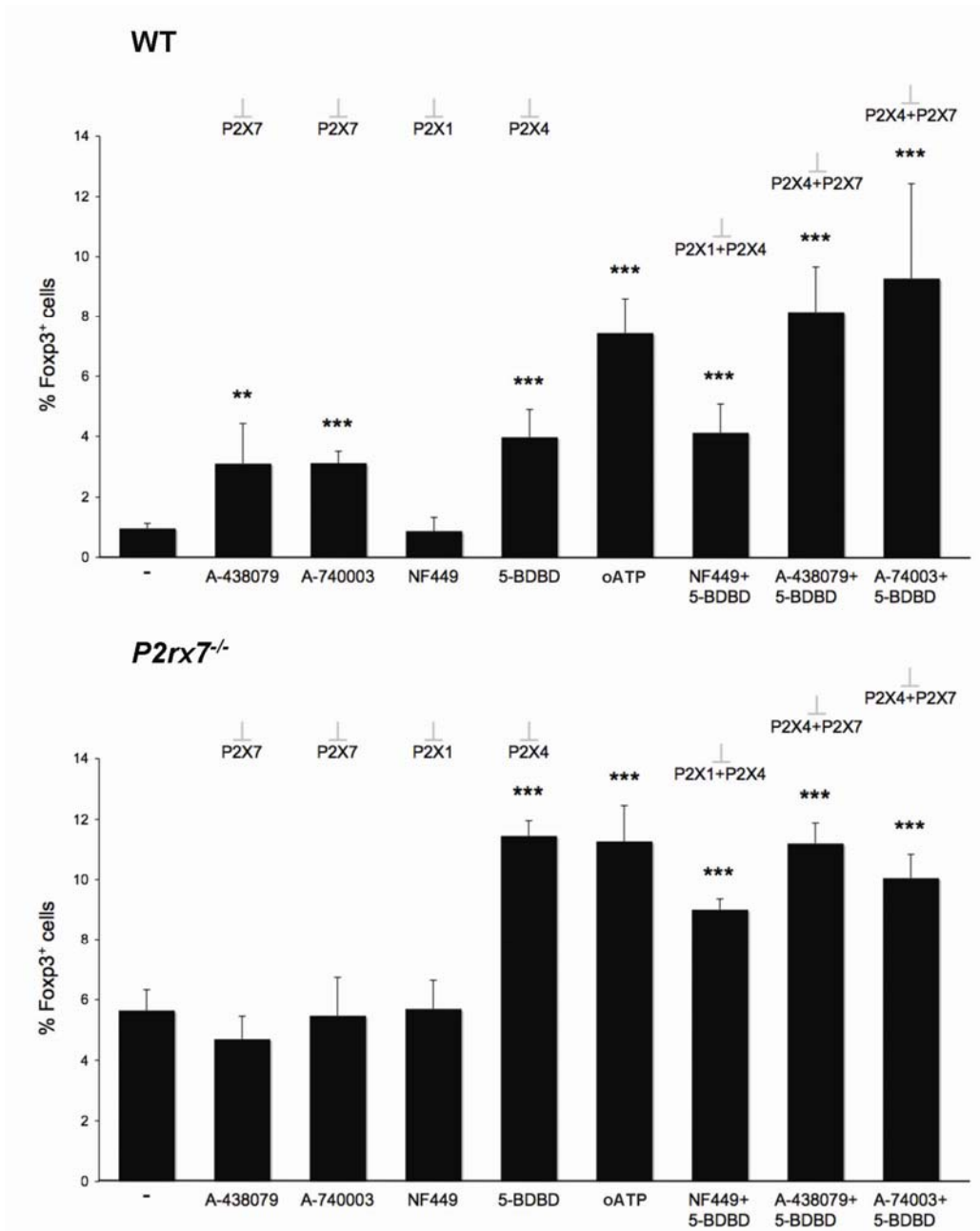


Fig. S6. Conversion of T_{conv} cells to T_{regs} by P2X antagonism. Flow cytometric determination of the percentages of $CD25^{high}Foxp3^{+}$ cells seven days after stimulation of naïve T cells from C57BL/6 and $p2rx7^{-/-}$ mice. Cells were stimulated for the first 48 hours with monoclonal antibody against CD3 and the indicated P2X antagonist(s) in the presence of irradiated splenocytes from $cd3e^{-/-}$ mice, and then they were maintained in IL-2 (50 U/ml). For selective antagonism of P2 receptors, the following compounds were used: NF449 (30 μ M) for P2X1; 5-BDBD (100 μ M) for P2X4; A-740003 (10 μ M) or A-438079 (10 μ M) for P2X7. All of the antagonists were from Tocris Bioscience. Statistical analysis was performed by the Student's t test. Mean values \pm SD are shown ($n = 4$ experiments; **, $P < 0.01$; ***, $P < 0.001$).

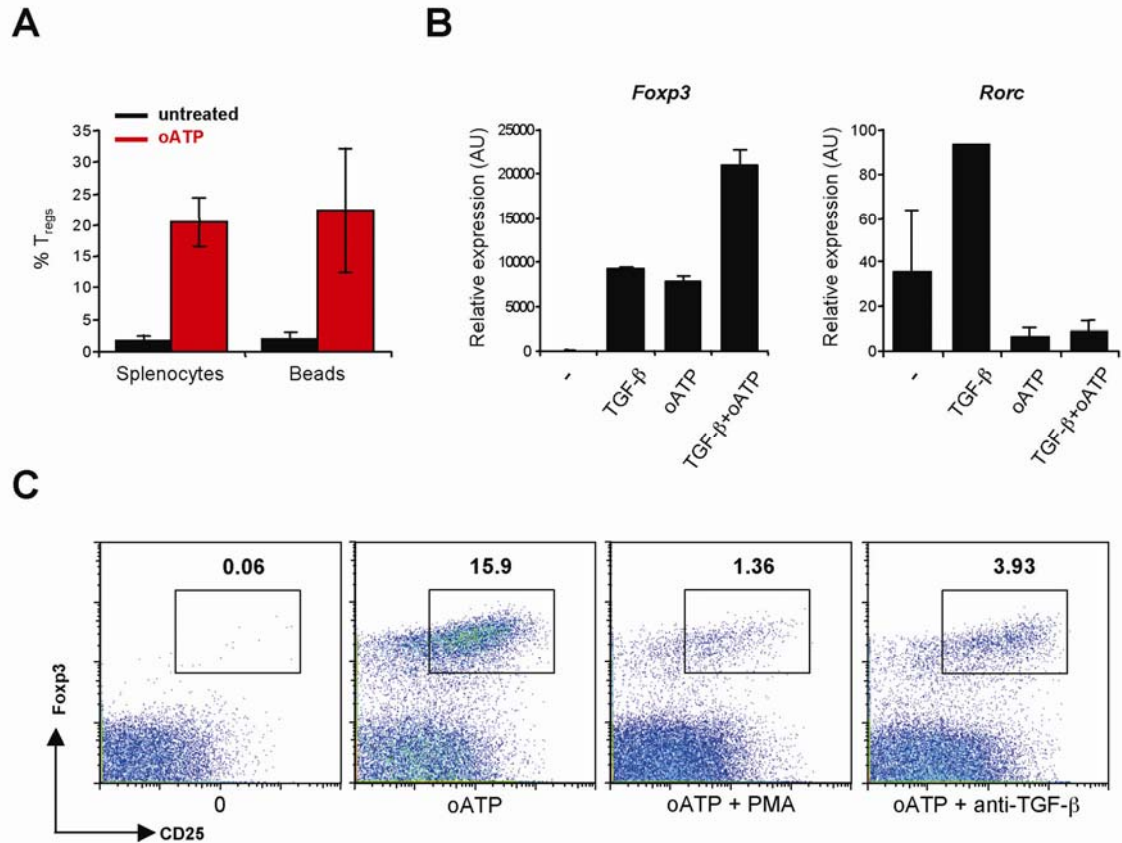


Fig. S7. Generation of T_{regs} by oATP and the additive effect of TGF- β . **(A)** Percentages of $CD4^+CD25^{\text{high}}Foxp3^+$ cells (T_{regs}) recovered at day 7 from naïve T cells that were stimulated for 48 hours with monoclonal antibody against CD3, together with irradiated splenocytes and IL-2 or microbeads coated with antibodies against CD3 and CD28. Black bars, control; red bars, oATP (100 μM). **(B)** RT-PCR analysis of the abundance of *Foxp3* and *Rorc* mRNAs from naïve T cells stimulated in the presence of the indicated agents. **(C)** Flow cytometric analysis of the abundances of CD25 and Foxp3 in naïve cells stimulated by monoclonal antibody against CD3, together with splenocytes and IL-2 as described earlier, in the presence of the indicated agents for the initial 48 hours of culture. Data are representative of at least three experiments.

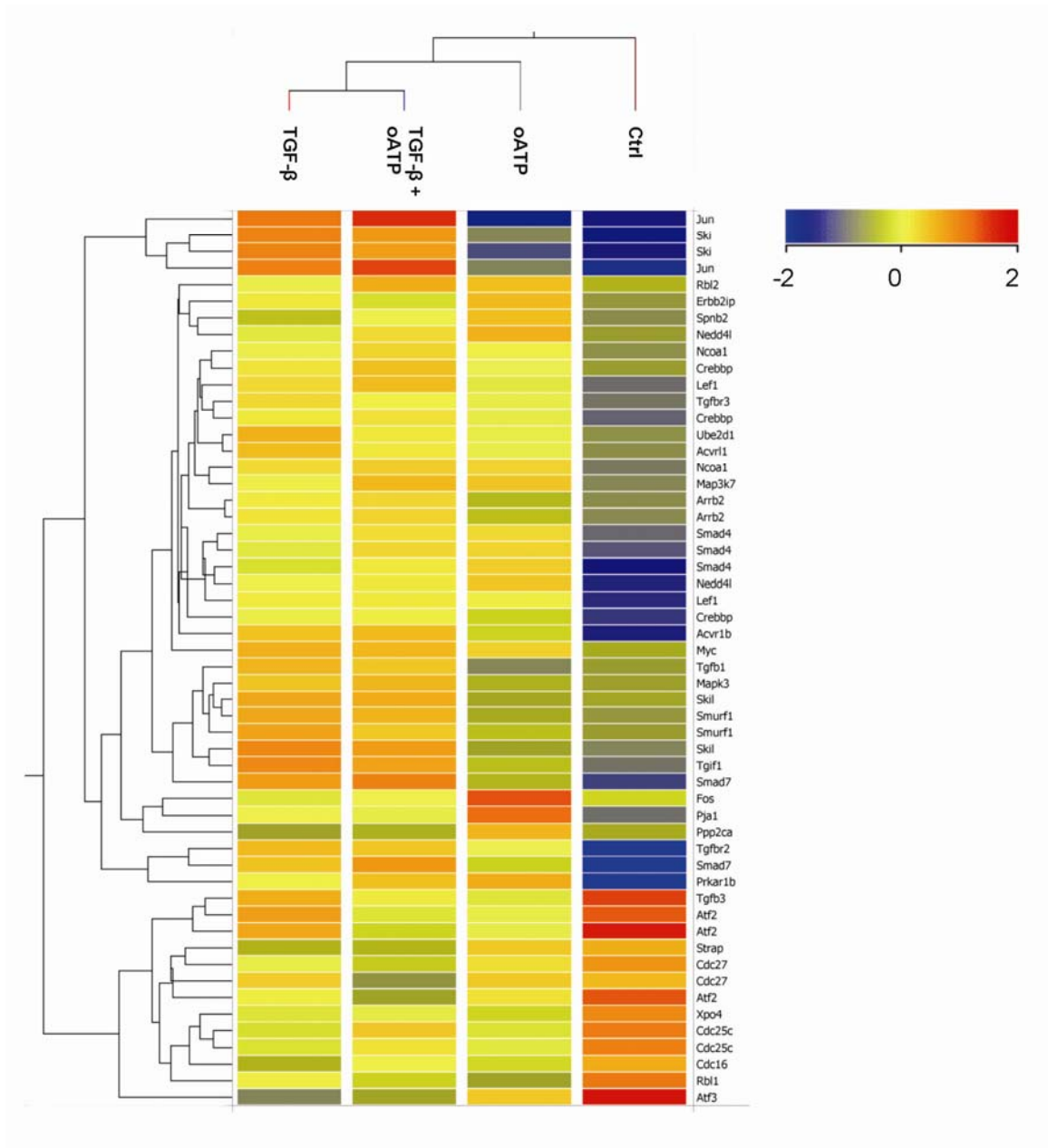


Fig. S8. Effects of TGF- β and oATP on the expression of genes whose products interact within the TGF- β pathway. The hierarchical cluster plot (<http://www.netpath.org>) shows the median centralized relative expression data of differentially expressed genes resulting from the comparison of untreated T_{conv} cells with T_{conv} cells that were treated with TGF- β , oATP, or TGF- β and oATP. Genes that exhibited a similar expression profile are clustered together (left tree), as are samples that showed a similar expression behavior within the TGF- β pathway (top tree).